Evaluating the Phagocytosis of Diseased Photoreceptor Outer Segments by Retinal Pigment Epithelial Cells in Age-Related Macular Degeneration

Madilyn Stahl

Abstract: Age-related macular degeneration (AMD), the leading cause of blindness in the elderly, is characterized by the death of photoreceptors and the retinal pigment epithelium (RPE). One of the main functions of the RPE is to phagocytose photoreceptor outer segments (POS) daily. While lipids in POS are used for energy production in the RPE, this process also produces toxic byproducts that cause oxidative damage. This study used induced pluripotent stem cells (iPSC) differentiated into RPE from a human donor without AMD (n = 1) to investigate whether photoreceptor disease state has an effect on the POS uptake. Results show that POS uptake is not dependent on AMD presence, but the uptake is POS donor specific.

1. Introduction

Age-related macular degeneration (AMD) is the leading cause of irreversible vision loss of the elderly in the developed world [1]. The global prevalence of AMD in 2020 was estimated to be 196 million cases and is expected to increase to 288 million by 2040 [2]. AMD causes distortion and loss of central vision, leading to blindness [1]. The disease is multifactorial in nature, involving a complex interplay between genetic and environmental factors [3]. Although there is no cure for AMD, the less common form, “wet” AMD, has treatment options to preserve vision including ocular injections to inhibit vascular endothelial growth factor (VEGF), the signal for producing more blood vessels [4]. There are currently no effective therapies for the more common form of the disease, “dry” AMD, which accounts for approximately 80% of AMD

cases [5]. Dry AMD is characterized by the death of light-sensing photoreceptors and the retinal pigment epithelium (RPE). Understanding why these cells die is an important first step for developing effective therapies.

The RPE is a monolayer of cells that forms the blood-retina barrier and has many functions for vision including absorbing light, transporting nutrients to photoreceptors, regenerating visual pigments, secreting growth factors to photoreceptors, and phagocytosing shed photoreceptor outer segments (POS) [6]. POS must be shed and continually renewed to eliminate toxic compounds in photoreceptor membranes and proteins caused by light damage. RPE cells are the only cell type to phagocytose daily for their entire life. Phagocytosing more material than any other cell type puts the RPE at a high risk for oxidative damage from the toxic waste products contained in the POS [7,8]. Phagocytosis of POS by the RPE involves three main steps, recognition, internalization, and digestion. RPE recognize phosphatidylserine, an “eat me” signal that is exposed on POS tips in a diurnal cycle [9]. Phosphatidylserine is primarily recognized by the αvβ5 integrin receptor on RPE cells, which involves additional extracellular bridge proteins. Following recognition by αvβ5, POS are internalized via the receptor tyrosine kinase Mer (MerTK), through a complex signaling mechanism that allows cytoskeleton and plasma membrane rearrangements for POS intake [10]. POS are degraded by phagolysosomes containing cathepsin D and S proteases [11].

While the mechanism for AMD is still unclear, previous reports from macular translocation, a surgical procedure that relocates a section of macular retina to healthy RPE show the recurrence of RPE atrophy beneath the relocated macula suggesting the diseased photoreceptors could contain molecules that are toxic to RPE [12].

In this study, we utilized a cell culture system since it provides a way to compare diseased and non-diseased POS in the same RPE. We hypothesize that the RPE will have decreased phagocytic uptake when fed diseased POS when compared to feeding of normal POS. To our knowledge, isolated human POS from donor eyes that have been graded for the presence and severity of AMD have not been used in phagocytosis experiments.

2. Materials and Methods

2.1 Human Eye Procurement and Grading for AMD

Donor eyes were obtained from Lions Gift of Sight (St. Paul, MN) and graded for AMD severity by a board-certified ophthalmologist (Dr. Sandra Montezuma) using the Minnesota Grading System (MGS). MGS 1 represents the control group with no AMD, and MGS 2, 3, and 4 are early, intermediate, and advanced AMD, respectively [13]. Eyes were obtained with consent from the donor family for medical research.

2.2 Culturing iPSC-RPE Cells

The derivation of induced pluripotent stem cell (iPSC) from human conjunctival cells and the differentiation into RPE was performed as previously described [14]. iPSC-RPE cells were cultured in Minimum Essential Medium Eagle alpha medium (MEMα; Sigma-Aldrich) supplemented with Glutamax, 5% FBS, N1 supplement, penicillin, streptomycin, non-essential amino acids, taurine, triiodothyronine, and hydrocortisone on 1X Matrigel (Corning) coated plates at 37°C, 5% CO_2, with two medium changes per week. Cells were dissociated with Accumax (Sigma-Aldrich) and passaged to confluency ($2x10^5$ cells/cm^2). Cells from passages 3-5 were used in all assays.

2.3 Purification of POS

The protocol for purification of POS was adapted from Parinot et al., 2014 [15]. POS were isolated from retinas of human donor eyes. A 25%-60% sucrose gradient was made in four steps by freezing each layer (25%, 36%, 48%, 60% sucrose, 20 mM tris acetate pH 7.2, 10 mM glucose, 5 mM taurine) in ice-cold methanol before adding the next, and then stored at -20°C. An hour before use, the gradients were thawed at 4°C. Crude retinal homogenates, each containing a quarter to half of a retina in homogenization buffer (20% sucrose, 20 mM tris acetate pH 7.2, 2 mM $MgCl_2$, 10 mM glucose, 5 mM taurine), were made by pulse vortexing at medium speed and passaging through a pipette tip with a cut tip. The retinal homogenates were layered on top of the sucrose gradient and placed in a centrifuge for one hour at 4°C using a Beckman MLS-50 Swinging-Bucket rotor at 32,000 rpm (100,000 x *g*). Purified POS were collected from the gradient interface in a single band, washed sequentially with wash 1 (20 mM tris acetate pH 7.2, 5 mM taurine), wash 2 (10% sucrose, 20 mM tris acetate pH 7.2, 5 mM taurine), wash 3 (10% sucrose, 20 mM sodium phosphate pH 7.2, 5 mM taurine), and counted using a hemocytometer as described in Parinot et al., 2014 [15]. Purified POS were stored in aliquots of 10 million POS at -80°C in MEMα media containing 2.5% sucrose.

2.4 POS Phagocytosis

Purified POS were labeled with FITC (fluorescein isothiocyanate isomer I; ThermoFisher), a fluorescent probe that labels amine groups. The solid FITC was reconstituted to 2.5 mg/mL in a sodium bicarbonate buffer (0.1 M sodium carbonate pH 9.5) by mixing for 1 hour while protected from light. After reconstitution, the POS pellet, containing approximately 10 million POS, was incubated for 1.5 hours while protected from light. Following the FITC incubation, labeled POS were washed using wash 3 (as described above) and resuspended in MEMα media as described in Parinot et al., 2014 [15]. The labeled POS were added to

confluent, adherent iPSC-RPE in a 48-well plate at a concentration of 10 POS/cell. The POS were incubated at 37°C, 5% CO_2 with the cells for different amounts of time. After incubation, cells were washed with Dulbecco's phosphate buffered saline (DPBS; ThermoFisher) containing Ca and Mg, then single cells were collected using Accumax. The cells were washed with DPBS without Ca and Mg and resuspended in 1% BSA in DPBS. Both bright field and fluorescent images were taken at 20x magnification using a Cytation 1 (BioTek) and Gen5 software (BioTek). Images were prepared using Fiji (ImageJ). Fluorescence-activated cell sorting (FACS) was performed using a BD LSRFortessa and the data was analyzed with FlowJo software.

2.5 Western Blotting

Membrane proteins from purified POS were solubilized using 30mM octylglucoside, 10mM tris acetate, and 5mM $MgCl_2$ pH 7.2. Following FACS analysis, cell pellets were collected and lysed in RIPA buffer. Protein concentrations were determined with the Bicinchoninic acid assay, using albumin as the standard. Proteins were resolved by SDS-PAGE on polyacrylamide gels made with 2,2,2-Trichloroethanol that when UV light activated allowed for visualization of protein. Proteins were transferred to low-fluorescence Polyvinylidene difluoride (PVDF) membranes using BioRad Turbo Blot, then imaged to normalize to protein load. Membranes were incubated overnight with a primary antibody, Rhodopsin (Abcam ab5417). Secondary antibodies conjugated to horseradish peroxidase along with the Chemiluminescence kit (ThermoFisher) were used to visualize the immune reactions. Images were taken using a BioRad ChemiDoc XRS. Densitometry was performed using Image Lab software (BioRad). Intensity of bands were normalized for protein load and to a standard run on each blot.

2.6 Statistical Analysis

Linear regression and t-tests were performed using GraphPad Prism 9 (GraphPad Software). $p \leq 0.05$ was considered statistically significant.

3. Results

3.1 Donor Demographics

The somatic cell source for the iPSC-RPE in this study were epithelial cells from the conjunctiva of human donor eyes. POS were isolated from human donor retinal tissue. Donor demographics and clinical information from the Lions Gift of Sight for iPSC-RPE generation and POS isolation used in this study is summarized in Table 1. The presence and severity of AMD was determined with high resolution retinal photomicrographs using the MGS [13]. Donors included those with no AMD (MGS1) and AMD (MGS2). The average age of donors used for POS isolation with no AMD (74 ± 10.3 years) and AMD (77 ± 2.5 years) is not significantly different ($p = 0.83$) by t-test comparison.

Table 1. Donor characteristics. [a]Age of donor in years. [b]Gender of donor. M = male, F = female. [c]MGS was used to evaluate the stage of AMD. MGS 1 = no disease, MGS 2 = early disease. [d]Time of death in military time.

Donor ID	Age[a]/Gender[b]	MGS Stage[c]	Cause of Death	Time of Death[d]	Use
MGS1-0027-1A3	80/M	1	Brain hemorrhage	21:02	Generation of iPSC-RPE
MGS1-0746	66/M	1	Cardiovascular collapse	1:01	POS isolation
MGS1-0949	82/F	1	Anoxic brain injury	18:50	POS isolation
MGS2-0833	83/F	2	Brain aneurysm	16:45	POS isolation
MGS2-0871	70/F	2	Natural	18:50	POS isolation

3.2 Characterization of POS

POS were isolated from human donor retinas using a sucrose gradient as described. Following centrifugation, a single band containing purified POS was obtained from the gradient interface at ~48% (Figure 1A). Preliminary characterization of POS was needed to ensure the quality of the preparation. Purified POS were imaged to calculate yield and analyze quality (Figure 1B, 1C). Our POS preparations exhibited both elongated and whirled forms (Figure 1B) [15]. The average POS yield per retina was $16.3 \times 10^6 \pm 3.3 \times 10^6$.

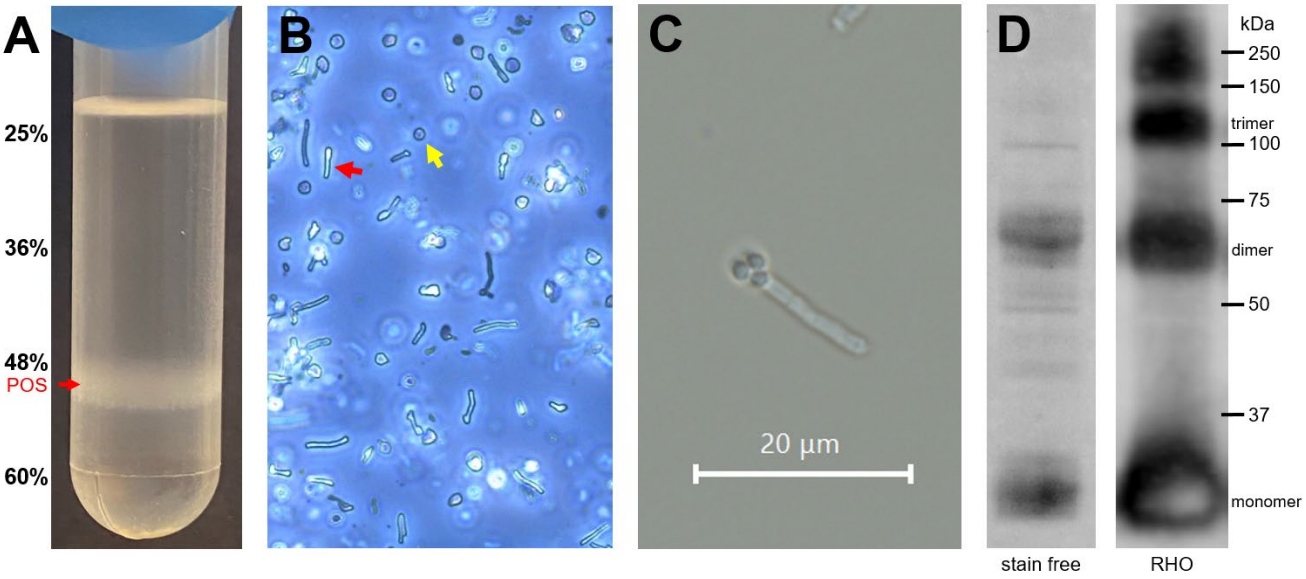

Figure 1. POS isolation. (A) Sucrose gradient from 25-60% containing the purified POS band around 48% sucrose. (B) Purified POS in trypan blue under 20X magnification. POS may be observed as elongated (red arrow) or whirled (yellow arrow) forms. (C) Purified POS under 60X magnification. Scale bar = 20µm. (D) Image of western blot showing rhodopsin content in purified POS. Rhodopsin bands (RHO) were normalized to stain free image of protein load.

To further characterize POS, disc membranes were disrupted with octylglucoside and rhodopsin content was analyzed via western blotting. Prior to detecting rhodopsin, a stain free image of the blot was taken to analyze all protein content of the POS preparation. Our preparation shows that the POS have multiple proteins, but rhodopsin is the major component

(Figure 1D). After detection of rhodopsin, abundant content was observed in our preparation of POS (Figure 1D). Multiple bands were observed, representing rhodopsin monomers, dimers, and trimers [16].

3.3 Phagocytosis of POS

iPSC-RPE were incubated with 10 FITC-labeled POS/cell from 1-6 hours to determine optimal timing for uptake. An additional overnight time point was used to get an estimate of the total number of RPE that phagocytose POS. Immediately before collecting single cells for FACS, bright field and fluorescent images were taken to ensure POS uptake by the iPSC-RPE (Figure 2A). FACS analysis was performed on single cells following POS incubation, and the percentage of cells containing FITC-labeled POS was determined (Figure 2B, 2C). The linear range of POS uptake was observed from 0-2 hours, with a plateau of uptake around 4 hours. The linear range of uptake was chosen to compare the effect of disease on phagocytosis. Following FACS, cell pellets were collected and lysed in RIPA buffer.

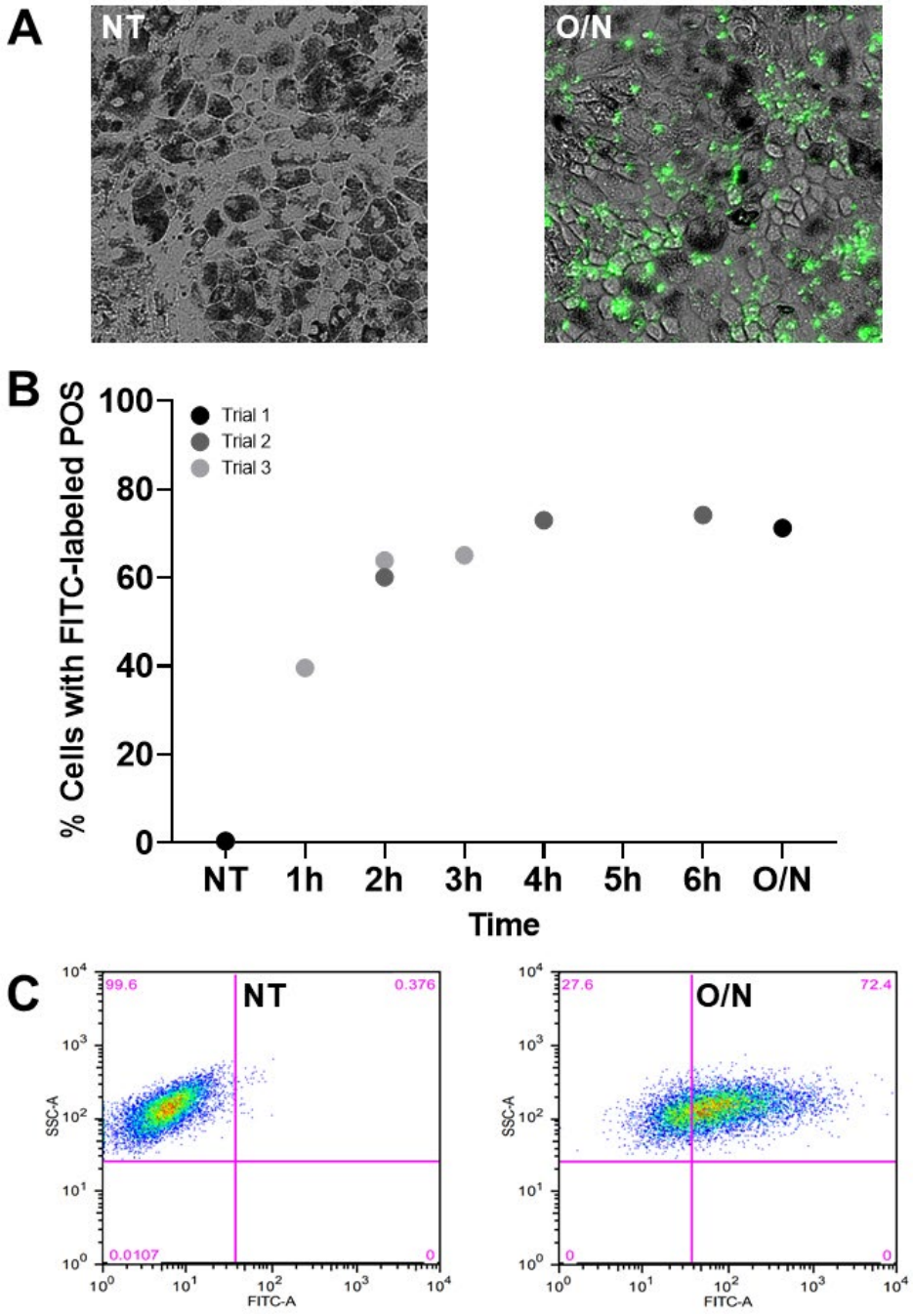

Figure 2. Functional analysis of POS. (A) Images of confluent iPSC-RPE without POS (NT) and after overnight incubation (O/N). (B) Graph showing preliminary FACS data from three different experiments. (C) Scatterplot from FACS of iPSC-RPE with and without POS. Upper right quadrant indicates percentage of RPE with internalized FITC-labeled POS. NT = no POS treatment, O/N = overnight POS treatment.

3.4 No Significant Difference in AMD POS Uptake

To determine if there are disease-dependent differences in the rates of POS uptake, we utilized the linear range of uptake from 0-2 hours. POS isolated from donors with (n = 2) and without (n = 2) AMD were fed to iPSC-RPE from the same donor for 0.75, 1.5, and 2.25 hours. Linear models were used to determine the rate because the slopes fit the data based on the R^2 values (Figure 3).

Comparison of diseased and non-diseased POS uptake was not significant; the uptake slope of POS without AMD was 5.214, while the AMD POS uptake slope was 6.937 (p = 0.3292) (Figure 3A). However, when comparing each POS donor separately, the slopes significantly differ from each other, because there is no overlap in the 95% confidence intervals (Figure 3B). Results indicate that uptake is dependent on the POS donor rather than the presence of AMD (Figure 3B).

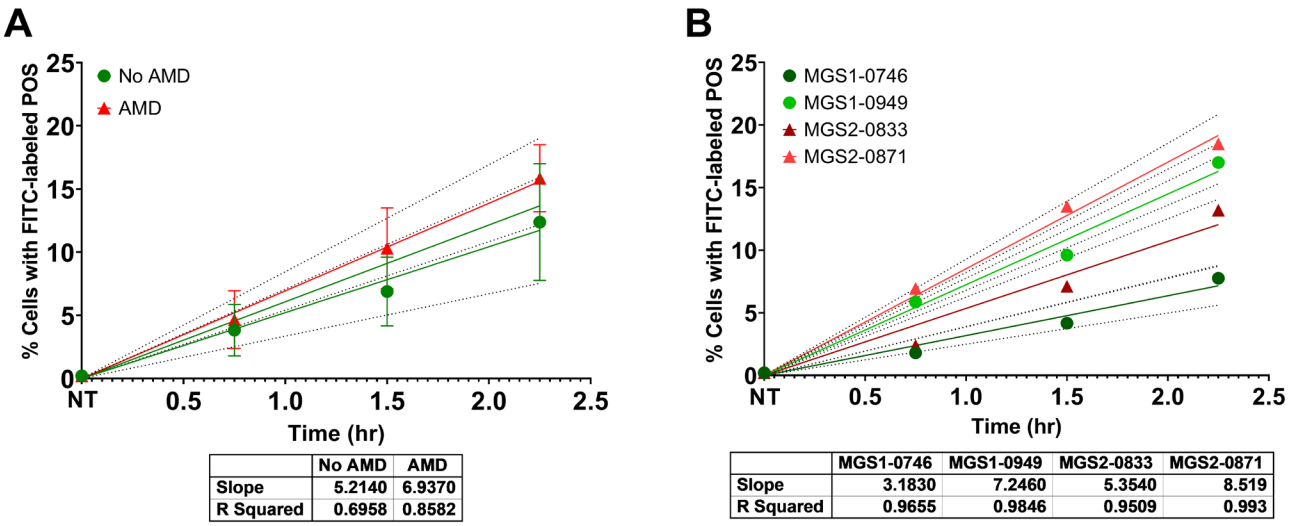

	No AMD	AMD
Slope	5.2140	6.9370
R Squared	0.6958	0.8582

	MGS1-0746	MGS1-0949	MGS2-0833	MGS2-0871
Slope	3.1830	7.2460	5.3540	8.519
R Squared	0.9655	0.9846	0.9509	0.993

Figure 3. Uptake of POS by iPSC-RPE. (A) Average uptake of no AMD and AMD POS. Data is presented as mean ± SEM. (B) Comparison of uptake for each individual POS donor. Data is presented as a single measurement of each sample. Tables summarize slope and R squared values. Dotted lines represent 95% confidence intervals.

To monitor rhodopsin degradation after phagocytosis, this experiment analyzed the rhodopsin C-terminus presence and disappearance. Previous work has established that the C-terminus of rhodopsin is degraded first in the RPE [17]. Following FACS analysis, the POS treated cells were collected and lysed for western blot analysis of rhodopsin (C-terminus) (Figure 4A). The content of the C-terminus of rhodopsin generally decreases over time (Figure 4B). When comparing rhodopsin content between AMD and no AMD POS treatment, the only statistically significant difference was observed at 1.5h.

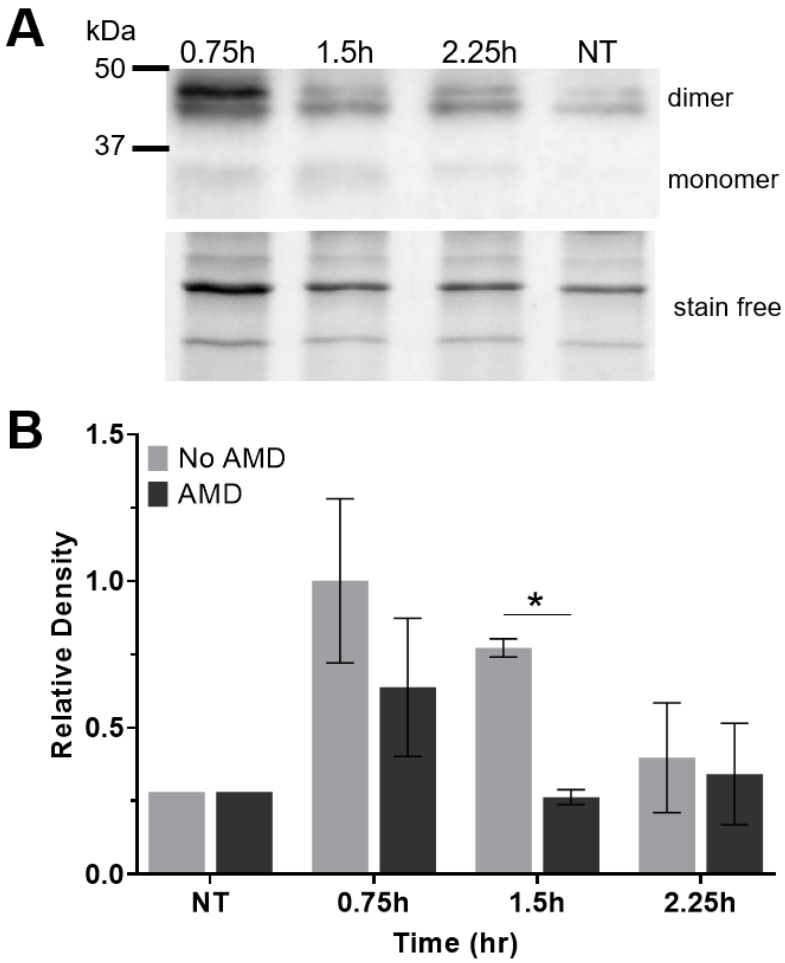

Figure 4. Western blot analysis of rhodopsin. (A) Representative image of western blots used to analyze rhodopsin content of iPSC-RPE after POS treatment and FACS analysis. Stain free image was used to normalize to protein load. (B) Average relative density of rhodopsin

(monomer and dimer) relative to no AMD 0.75h. An unpaired t-test was used to compare disease status. Data is presented as mean ± SEM. * $p < 0.05$ determined by unpaired t-tests comparing disease vs no disease. NT = no POS treatment.

4. Discussion

In this study, we used purified POS isolated from human donors graded for the presence and severity of AMD. This model system allowed comparison of the feeding of diseased or non-diseased POS to iPSC-RPE cells in culture. Our results show that there is no significant difference in the uptake of AMD vs no AMD POS by iPSC-RPE (Figure 3A). However, there is a significant difference in the phagocytosis rate of each individual POS donor (Figure 3B). Rhodopsin content after FACS analysis showed that the POS were being degraded by the RPE over time (Figure 4).

The difference in individual donor POS uptake may relate to the complex mechanism of phagocytosis. The key molecule present in POS, phosphatidylserine, is exposed on the POS tips in a diurnal rhythm, suggesting the time of death of the donor may affect how well the iPSC-RPE can recognize and internalize the POS [9]. For example, MGS1-0746 had the lowest uptake slope with the time of death at 1am. The other three POS donors had a time of death in the early evening, with uptake averaging about 2-fold faster. A future direction for this study would be to analyze the phosphatidylserine content by mass spectroscopy in our POS preparations and analyze if the time of death is a factor in our phagocytosis experiments.

Analysis of POS uptake based on FACS shows no difference based on disease state of the POS donor. However, analysis of rhodopsin content after POS treatments showed a significant difference between AMD and no AMD POS treatment at 1.5h. This significant difference in

rhodopsin content suggests degradation of POS could be disease dependent. However, these results reflect the competing actions of uptake and degradation, so additional experiments may have to be utilized to uncover other mechanisms involved. Future studies will continue to investigate the degradation of POS and the effect of disease status.

The limitations of this study include the low number of samples and variable time of death of the donors, which could have affected the uptake of POS. This study also used one iPSC-RPE donor without AMD, so the disease state of RPE with the same POS was not compared. Previous studies on AMD RPE have shown decreased mitochondrial function and dysfunctional autophagy, which are both connected to phagocytosis [18,19]. Disease state of RPE may also alter the uptake and degradation of POS.

In summary, our results show that there is no difference in POS uptake by iPSC-RPE when comparing disease status of POS. When comparing individual donors, rates of phagocytosis are significantly different. Analysis of rhodopsin content in cells after POS treatment shows a significant difference between AMD and no AMD at 1.5h. These results suggest factors other than disease, such as phosphatidylserine content of POS, could influence the uptake.

Funding: This research was supported by the Undergraduate Research Opportunities Program (UROP).

Acknowledgements: I am sincerely grateful to Dr. Deborah Ferrington for the guidance and support throughout this project. I wish to acknowledge the Lions Gift of Sight personnel for the procurement, photographing, and processing of eye tissue. I would like to acknowledge the

assistance of Becky Kapphahn in experiment design, Zhaohui Geng in FACS analysis, and Mara Supik and Cody Fisher in cell culture training.

References

1. Cheung, L.K.; Eaton, A. Age-related macular degeneration. *Pharmacother. J. Hum. Pharmacol. Drug Ther.* **2013**, *33*, 838–855, doi:10.1002/phar.1264.
2. Wong, W.L.; Su, X.; Li, X.; Cheung, C.M.G.; Klein, R.; Cheng, C.-Y.; Wong, T.Y. Global prevalence of age-related macular degeneration and disease burden projection for 2020 and 2040: A systematic review and meta-analysis. *Lancet. Glob. Heal.* **2014**, *2*, e106-16, doi:10.1016/S2214-109X(13)70145-1.
3. Chakravarthy, U.; Wong, T.Y.; Fletcher, A.; Piault, E.; Evans, C.; Zlateva, G.; Buggage, R.; Pleil, A.; Mitchell, P. Clinical risk factors for age-related macular degeneration: A systematic review and meta-analysis. *BMC Ophthalmol.* **2010**, *10*, 31, doi:10.1186/1471-2415-10-31.
4. Brown, D.; Heier, J.S.; Boyer, D.S.; Freund, K.B.; Kaiser, P.; Kim, J.E.; Sarraf, D. Current best clinical practices—Management of neovascular AMD. *J. Vitreoretin. Dis.* **2017**, *1*, 294–297, doi:10.1177/2474126417725946.
5. Ferrington, D.A.; Fisher, C.R.; Kowluru, R.A. Mitochondrial defects drive degenerative retinal diseases. *Trends Mol. Med.* **2020**, *26*, 105–118, doi:10.1016/j.molmed.2019.10.008.
6. Strauss, O. The retinal pigment epithelium in visual function. *Physiol. Rev.* **2005**, *85*, 845–881, doi:10.1152/physrev.00021.2004.
7. Kevany, B.M.; Palczewski, K. Phagocytosis of retinal rod and cone photoreceptors.

Physiology **2010**, *25*, 8–15, doi:10.1152/physiol.00038.2009.

8. Mazzoni, F.; Safa, H.; Finnemann, S.C. Understanding photoreceptor outer segment phagocytosis: Use and utility of RPE cells in culture. *Exp. Eye Res.* **2014**, *126*, 51–60, doi:10.1016/j.exer.2014.01.010.
9. Ruggiero, L.; Connor, M.P.; Chen, J.; Langen, R.; Finnemann, S.C. Diurnal, localized exposure of phosphatidylserine by rod outer segment tips in wild-type but not Itgb5-/- or Mfge8-/- mouse retina. *Proc. Natl. Acad. Sci.* **2012**, *109*, 8145–8148, doi:10.1073/pnas.1121101109.
10. Müller, C.; Finnemann, S.C. RPE Phagocytosis. In *Retinal Pigment Epithelium in Health and Disease*; Springer International Publishing: Cham, 2020; pp. 47–63.
11. Rakoczy, P.E.; Mann, K.; Cavaney, D.M.; Robertson, T.; Papadimitreou, J.; Constable, I.J. Detection and possible functions of a cysteine protease involved in digestion of rod outer segments by retinal pigment epithelial cells. *Invest. Ophthalmol. Vis. Sci.* **1994**, *35*, 4100–8.
12. Cahill, M.T. Recurrence of retinal pigment epithelial changes after macular translocation with 360° peripheral retinectomy for geographic atrophy. *Arch. Ophthalmol.* **2005**, *123*, 935, doi:10.1001/archopht.123.7.935.
13. Olsen, T.W.; Feng, X. The Minnesota Grading System of eye bank eyes for age-related macular degeneration. *Investig. Ophthalmol. Vis. Sci.* **2004**, *45*, 4484–4490, doi:10.1167/iovs.04-0342.
14. Geng, Z.; Walsh, P.J.; Truong, V.; Hill, C.; Ebeling, M.; Kapphahn, R.J.; Montezuma, S.R.; Yuan, C.; Roehrich, H.; Ferrington, D.A.; et al. Generation of retinal pigmented epithelium from iPSCs derived from the conjunctiva of donors with and without age

related macular degeneration. *PLoS One* **2017**, *12*, e0173575, doi:10.1371/journal.pone.0173575.

15. Parinot, C.; Rieu, Q.; Chatagnon, J.; Finnemann, S.C.; Nandrot, E.F. Large-scale purification of porcine or bovine photoreceptor outer segments for phagocytosis assays on retinal pigment epithelial cells. *J. Vis. Exp.* **2014**, doi:10.3791/52100.
16. Zhang, T.; Cao, L.-H.; Kumar, S.; Enemchukwu, N.O.; Zhang, N.; Lambert, A.; Zhao, X.; Jones, A.; Wang, S.; Dennis, E.M.; et al. Dimerization of visual pigments in vivo. *Proc. Natl. Acad. Sci.* **2016**, *113*, 9093–9098, doi:10.1073/pnas.1609018113.
17. Wavre-Shapton, S.T.; Meschede, I.P.; Seabra, M.C.; Futter, C.E. Phagosome maturation during endosome interaction revealed by partial rhodopsin processing in retinal pigment epithelium. *J. Cell Sci.* **2014**, doi:10.1242/jcs.154757.
18. Ferrington, D.A.; Ebeling, M.C.; Kapphahn, R.J.; Terluk, M.R.; Fisher, C.R.; Polanco, J.R.; Roehrich, H.; Leary, M.M.; Geng, Z.; Dutton, J.R.; et al. Altered bioenergetics and enhanced resistance to oxidative stress in human retinal pigment epithelial cells from donors with age-related macular degeneration. *Redox Biol.* **2017**, *13*, 255–265, doi:10.1016/j.redox.2017.05.015.
19. Golestaneh, N.; Chu, Y.; Xiao, Y.-Y.; Stoleru, G.L.; Theos, A.C. Dysfunctional autophagy in RPE, a contributing factor in age-related macular degeneration. *Cell Death Dis.* **2018**, *8*, e2537–e2537, doi:10.1038/cddis.2016.453.